10th Pacific Symposium on Flow Visualization and Image Processing
Naples, Italy, 15-18 June, 2015

Image processing to study the evolution of channel slope and water depth in bimodal sediment mixtures

Hugo Lafaye de Micheaux[1,2,4,*], Ashley Dudill[1,2,3], Philippe Frey[1,2], Christophe Ducottet[4]

[1]Irstea, Unité de Recherche Erosion Torrentielle Neige et Avalanches, Grenoble, France
[2]Univ. Grenoble Alpes, Grenoble, France
[3]Department of Geography, University of British Columbia, Vancouver, Canada
[4]Laboratoire Hubert Curien, CNRS UMR5516, Université de Saint-Etienne, Université de Lyon, Saint-Etienne, France
[*]corresponding author: hugo.lafaye-de-micheaux@irstea.fr

Abstract Bedload transport is the sediment load transported in contact with the bed of a river channel. Empirical relations are often used to predict sediment transport rates. However, these predictions usually lack accuracy. Consequently, a more detailed comprehension of the physical processes is required. For example, we require an improved understanding on how fine sediment inputs to river channels influence sediment transport, channel stability, ecology and stratigraphy. In this context, an experimental investigation was undertaken in a laboratory flume equipped with controlled water and sediment supplies to create bimodal mixtures of coarse and fine spherical glass beads. The flume experiments were recorded using a high frequency camera. We propose a new image analysis chain dedicated to automatically detect the water free surface and the bed elevation for a sequence of images. This method is based on a combination of morphological operations, gradient calculations and watershed transformations. The detections allowed the measurement of important physical quantities such as water depth, slope and their evolution over time. By making comparisons for varying sizes of fine sediment, we have highlighted several phenomena which permit a better understanding of bedload mobility, specifically related to the influence of grain size ratio.
Keywords: bedload, sediment transport, segregation, experimental flume, image analysis, line detection, marker-controlled watershed

1 Introduction

The transport of sediment through river channels has major consequences for public safety, management of water resources, and environmental sustainability. Most studies of sediment transport in rivers have focused on mass flux and its relation to water flow. But there is still no satisfactory theory for bedload transport, the sediment load transported in contact with the stream bed. Viewing bedload as a granular phenomenon may provide a better insight [1].

It is well known that when grains of different sizes are subjected to a shear flow, such as in a gravel-bed river, they will segregate, leading to fluvial morphological features [2]. There are different mechanisms of vertical size segregation: spontaneous percolation when fine sediment arrives in a static coarse sediment bed and falls into the voids between grains, and kinetic sieving when fine sediment arrives in a coarse sediment bed in motion and falls into voids which become dynamically available between the moving coarse grains. Both are influenced by the grain size ratio between the coarse sediment bed and the infiltrating finer sediment [3]. This paper will focus on kinetic sieving only.

We simulated a fluvial context, in a highly simplified manner through the use of an experimental laboratory, similar to the setup described in [4], using spherical beads and a narrow channel. We introduced a small concentration of fine beads into a bed formed solely of larger beads in equilibrium (input rate = output rate); this allowed us to visualise the segregation process. By varying the size of the fine beads, we were able to change the grain size ratio, and observe the influence upon segregation response.

The goal of this paper is to propose a new image analysis chain dedicated to automatically detect the water free surface and the bed elevation for a sequence of images. More precisely, this method allows to study over time the boundary of two main regions involved in sediment transport: the stable bed and the mobile bed. Each boundary is detected in the form of horizontal lines in the observation window. The innovation here was to mix morphological operations with a combination of gradient calculations and watershed transformations [6]

to detect those lines. The detected lines were then used to study the channel slope and water depth evolution over time for different grain size ratios.

The paper is structured as follows: first, we present the experimental facilities and procedure, and show what type of data is processed; then, after positioning the problem, we describe the image processing algorithm used to detect the bed and water free surface, and how we validate the results of the algorithm; finally, we study the channel slope and the water depth evolution over time for different grain size ratios.

2 Experimental study

The experiments were undertaken at IRSTEA (Institut National de Recherche en Sciences et Technologies pour l'Environnement et l'Agriculture), Centre de Grenoble, France. They were highly simplified and allowed clear visualisation of the phenomena and investigation at the scale of the particle.

2.1 Experimental setup

Facilities. The experimental setup consisted of a 2 m long, 10.3 mm wide, glass-sided flume set at a slope of 10.1 %. In order to cause bed formation, a 6.4 cm obstacle was placed at the channel outlet. The base of the flume is composed of different combinations of steel half cylinders, randomly arranged at different levels. The random arrangement of the bed prevents the occurrence of geometrically regular lattice (crystallographic) arrangements within the channel. This setup (Fig. 1) was also used by *Hergault et al.* [4] but had been widened to better study the infiltration of fine particles.

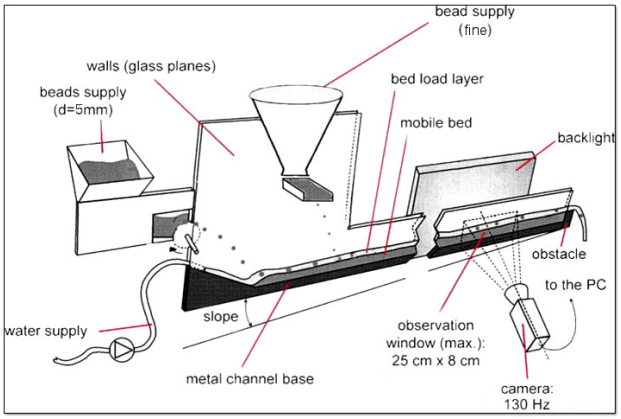

Fig. 1 A schematic diagram of the experimental flume for bimodal sediment mixture (after [4])

The bimodal sediment mixture was obtained by feeding coarse and fine spherical glass beads from two different bead distributors. The coarse bead diameter was 5 mm and the fine one was variable (0.7 mm, 0.9 mm, 1.5 mm, 2 mm, 3 mm and 4 mm) to modify the grain size ratio. All beads had a density of 2500 kg/m^3.

The flume walls were made of glass in order to allow individual and bulk grain movements to be clearly visualised and tracked; this was done using a black and white partial scan motion camera. This Photonfocus motion camera was placed perpendicular to the glass planes of the flume, and inclined at the same angle. It was operated at a resolution of 1024 x 500 pixels and a frame rate of 130 frames/second. Stable and uniform backlighting for the camera was provided by a LED panel on the opposite side of the flume.

Parameters. The water flow was turbulent and supercritical. Flow rate and coarse particle transport rate were kept constant at respective values of 0.0495 liter/s (4.80 l/s/m) and 8 kg/hr ($8.63.10^{-2}$ l/s/m). For all experiments with different diameters presented in this paper, the fine particle rate was also kept constant at approximately 2.3 kg/hr, which represented 22.2% of the total feed (coarse plus fine). The high slope of the flume resulted in a low water depth, and a low submergence ratio (water depth to bead diameter). The Shields number was approximately 0.09, *i.e.* about twice the threshold for incipient motion, at the beginning of the experiment, before the fine sediment was introduced.

2.2 Experimental procedure

During the experiments, coarse grains were in motion, so that fine grains fell into dynamically available open spaces ('kinetic sieving' process). First, the coarse sediment and water feeds were turned on to build up the bed to the height of the obstacle at the channel outlet. Experiments were undertaken in 'equilibrium' conditions, meaning that the bed slope was constant and that the feed rate was equal to the transport rate over a long time period. Once the coarse sediment was in transport equilibrium, the fine feed was introduced. Meanwhile, a sequence of images was taken using the camera so that the interaction between the fine and coarse sediments could be visualised. The experiment ran until a new equilibrium was reached (lasted approximately 18-20 minutes). This new equilibrium was characterized either by a lower (degradation) or higher (aggradation) bed slope. The experiment was repeated for each size of fine sediment.

2.3 Data type

Data obtained during the recording of the infiltration period formed a ≈20-minute sequence of black&white images (Fig. 2) at 130 frames/second. For the study reported in this paper, we did not need that many images. After the infiltration of the fine sediment into the coarse bed was nearly complete, the fine sediment formed a moving carpet-like layer of variable thickness above which coarse particles were essentially rolling (except in the 4 mm case).We kept only one image per second. So, the sequence was composed of ≈1200 images of size 1024 x 500 pixels. On images, the coarse sediment was transparent and the fine appeared in dark gray (except the 3 mm and 4 mm fine beads, which appeared as black and transparent, respectively). The upper dark line was the water free surface. The steel base of the flume can be seen with a dark color.

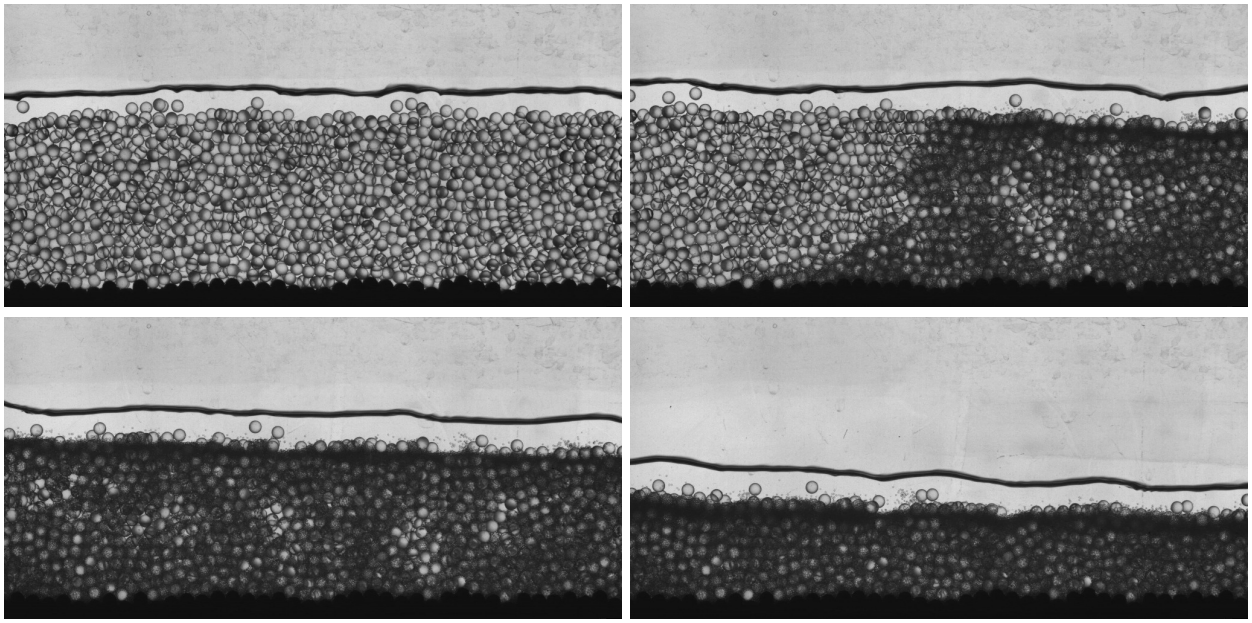

Fig. 2 Example of images from a sequence obtained with the experimental flume showing the evolution of the bed during the infiltration of fine particles of 0.7 mm. Images appeared respectively (from top left to bottom right) at: 0 min, 5 min, 7 min, 20 min. Flow from right to left.

3 Detection of bed line and water line

3.1 Positioning of the problem

An image processing algorithm was developed to evaluate the evolution of the channel over time. Image processing allows the computation of a high number of operations efficiently on many images with high precision. In this work, the aim was to extract the boundaries of the principal regions appearing in sediment transport (Fig. 3):

- the base line which is the limit between the fixed bottom bed and the evolving bed (yellow to blue boundary on Fig. 3),
- the bed line which is the limit between the evolving bed and the water flow (blue to green boundary on Fig. 3),
- the water line which is the limit between the evolving bed and the upper external air (green to red boundary on Fig. 3).

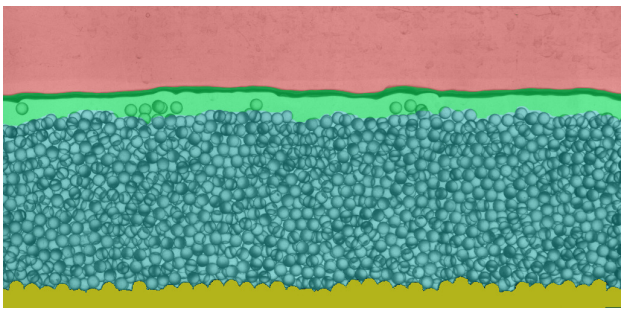

Fig. 3 Position of the 4 distinct regions in the images: the fixed base (yellow) corresponds to random half-cylinders; the mobile bed (blue) corresponds to the quasi-immobile beads composing the bed; the water flow (green) contains the fluid and the fast moving objects; the upper part is the air (red).

Classically such segmentation problems can be solved using either contour detection or region segmentation. Many algorithms can be used but here we have chosen a morphological approach based on the watershed transformation [6]. This approach basically consists in computing the modulus of the gradient and then to detect the crest line separating two basins located on either side of the line. A great advantage of the method is that it provides the detection of a single connected line thanks to the definition of relevant markers used as flooding sources.

The combination of morphological watershed and gradient is a powerful segmentation method first introduced by *Beucher et al.* [6] and refined in different works ([7] or [8]). It relies on the use of the watershed transformation which determines the boundaries of adjacent objects as ridges. To avoid oversegmentation, the watershed is applied on the gradient of the image and is based on a set of markers. This method was successfully used in many segmentation problems such as road segmentation [10], video segmentation [11] and medical image segmentation [12].

3.2 Algorithm description

To detect the bed surface and the water free surface on the images, we first detected the position of the base line on the first image of the sequence. Then, on each image, we removed the moving beads with a background extraction algorithm. Finally, we estimated the bed line and the water line positions.

Base line detection. The first step of the algorithm was to detect the base line. This was done only once - on the first image - and was subsequently used for all the images of the sequence. The principle of this algorithm was to apply a binary threshold to detect the fixed base region. Then, the upper boundary of this region was obtained by simple binary morphological operations. Although the fixed base was the darker region of the image, we had to remove the contribution of the water line and the mobile bed which were also dark. This was done using pre-processing. We proceeded with the following steps illustrated in Fig. 4:

1. Apply a morphological closing to the first image of the sequence (Fig. 4b). A vertical line was used as a structuring element, just long enough to remove the water free surface. The height of the line is denoted h. In our setup, the optimal value to remove the water surface was $h = 18$ pixels.
2. Filter the obtained image with a Gaussian filter of standard deviation σ to get rid of fine details and noise (Fig. 4c). The noise was mainly due to the transparent beads in the bed which was successfully removed by taking $\sigma = 3$ pixels.

3. Threshold the Gaussian filtered image (Fig. 4d). The threshold was automatically set to the first peak of the pixel intensity histogram to remove unwanted gray parts.
4. Dilate the binary image with a vertical line of 2 pixels as a structuring element.
5. Subtract the binary image formed in point 3. from the dilated image to highlight the edges between black and white (Fig. 4e). The resulting image gave the base line position.

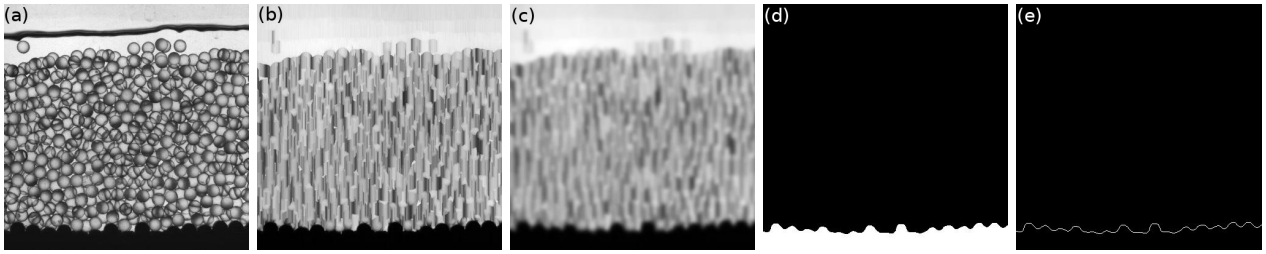

Fig. 4 Steps of the base line detection algorithm. **a** original image, **b** morphologically closed image, **c** filtered image, **d** thresholded image, **e** final result after subtracting image (d) from its dilatation.

Background extraction. The second step was to calculate the background of an image by averaging over P consecutive images (starting $(P-1)/2$ images before and ending $(P-1)/2$ after the current image). The effect of the averaging is to remove the moving bed which consists of all the beads moving during the time interval around the current image (see Fig. 5b). The number P of images was chosen to be a good compromise between having enough images to have a good map of moving particles, but not too many which would result in information at the bed surface being lost. In experiments, a value of $P = 30$ was chosen because it covered 30 seconds of the experiment.

Bed line detection. The third step was to detect the bed line on the background image. Here, the principle was to detect the line by computing a Sobel gradient [9] and to detect the crest line of this gradient through a marker based watershed transformation. As for the base line detection, some pre-processing steps were undertaken. The procedure, illustrated in Fig. 5, was:

1. Apply a morphological closing to the background image using a vertical line of height $h = 18$ pixels as a structuring element to remove the water free surface (Fig. 5c).
2. Filter the obtained image with a Gaussian filter of standard deviation $\sigma = 3$ pixels to get rid of fine details and noise (Fig. 5d).
3. Calculate the vertical gradient on the Gaussian filtered image (Fig. 5e). A vertical Sobel gradient operator was used here to see vertical variations in pixel intensity.
4. Compute the watershed transformation on the complement of the gradient image with the top of the image and the base line as markers (Fig. 5f). The resulting image gave the bed surface position.

Water line detection. The last step was the detection of the water line. As for the bed line, the idea was to compute a watershed transformation to detect the water line as the crest line of the free surface region. For that, we need a grayscale image with high values on the free surface region. Starting from the results obtained after the bed line detection, we proposed the following process:

5. Subtract the original image from the Gaussian filtered image obtained at point 2 of the bed line detection (Fig. 5g). The resulting image showed high pixel values near and on the water free surface.
6. Compute the watershed transformation with the top of the image and the bed line as markers (Fig. 5h). The resulting image gave the water free surface position.

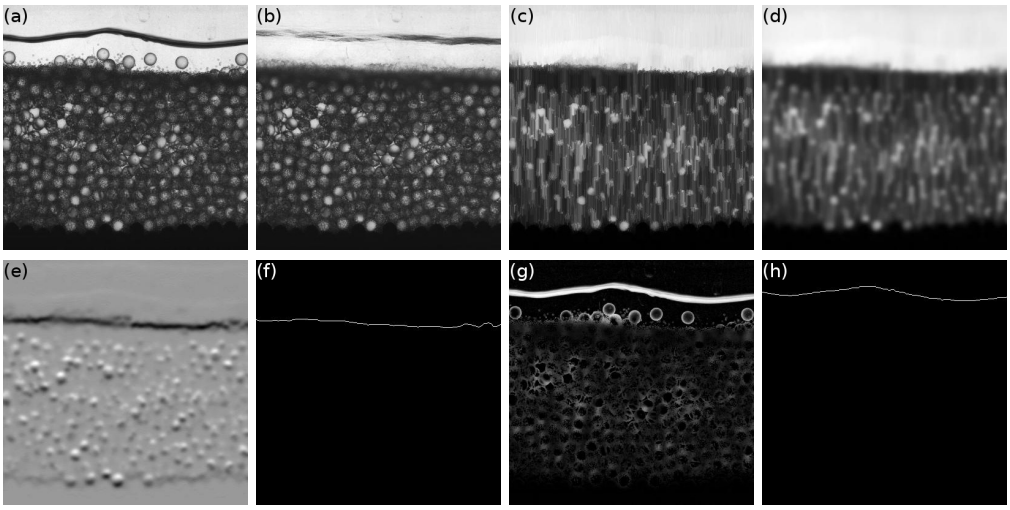

Fig. 5 Steps of the bed line and water line detection algorithms. **a** original image, **b** background image **c** morphological close of the background image, **d** filter of the closed image, **e** gradient of the filtered image, **f** result of the watershed transformation applied on the complement of the gradient image, **g** image obtained by subtracting the original image (a) from the filtered image (d), **h** result of the watershed transformation applied on the image (g).

3.3 Validation

In this section, we present two ways to validate the results of our algorithms: one way is based on the visual check of the detected lines, the other way is a statistical evaluation.

Visually. One method to validate the results was to check the detected lines visually. We created a sequence of images where the three detected lines - base, bed and water line - were all superimposed on the corresponding image. It allowed us to verify the precision of the position of the detected lines with the naked eye. In Fig. 6, we can see examples of line detections where the three lines appear to be well detected. But with this method, we could not review the whole sequence as it was more than 1000 images long.

Statistically. A second method to verify the integrity of the results was to use descriptive statistics along the whole sequence. Here we calculated the mean elevation of the detected bed line for each image of the sequence together with the standard deviation and the local standard deviation. By keeping only the maximum value of the local standard deviations, we were able to detect if bad detections occurred (a high value would correspond to a jump in the line and so would reveal probably an error). In Fig. 7, we can see two graphs with these values applied on the sequences where fine beads of 0.7 mm and 4 mm were introduced. We made the same graph for all other sequences to conclude that there were apparently no errors in the bed line detections (no high isolated peaks in the graphs). In the 4 mm case, we can see higher maximum local standard deviations which was due to the nature of the fine sediment layer on the bed surface. In this case, the bed surface was more irregular (due to the small grain size ratio) and therefore the detector was less accurate.

4 Results

In this section, we present the results obtained and the analysis performed using our algorithms. To understand why we concentrated our study on the channel slope and the water depth, let's consider the real case of sediment transport. In mountains, torrents adapt their slope, depth and width to maintain a balance between the water and sediment supplied from upstream, and transported downstream. When catastrophic floods occur, a huge quantity sediment is transported in mountain streams which may impact their stability. According to the size and the grain size distribution of these sediments, the impact on the streams may result in different modifications in slope, depth and width. These modifications are what we aim to understand. In our experimental setup, the width could not vary, so we focused our study on the channel slope and water depth.

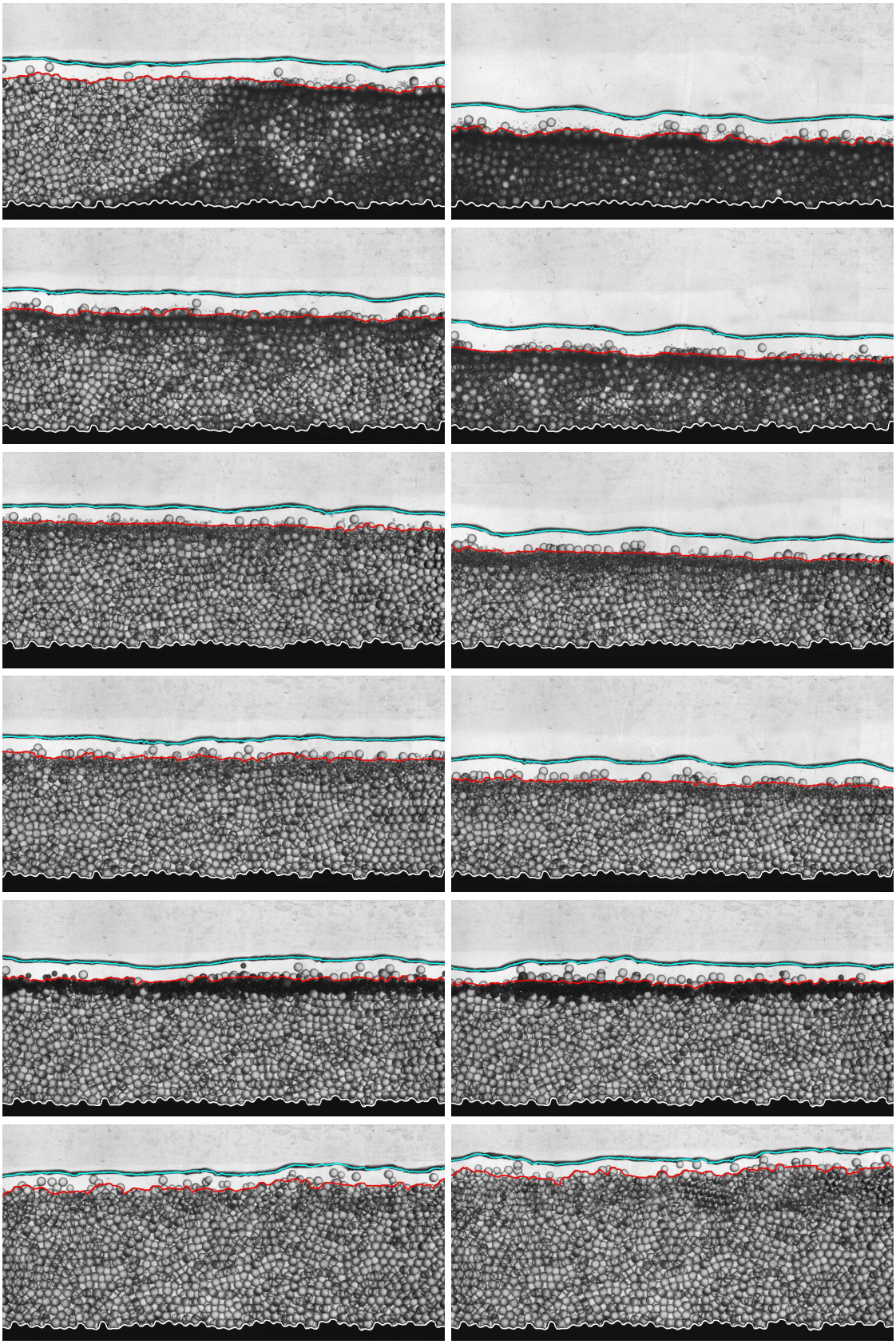

Fig. 6 Examples of detected base line (in white), bed line (in red) and water line (in cyan) superimposed on the corresponding image at 5 min (left column) and 15 min (right column) during the infiltration of fine beads of 0.7 mm, 0.9 mm, 1.5 mm, 2 mm, 3 mm and 4 mm (respectively in this order from top to down).

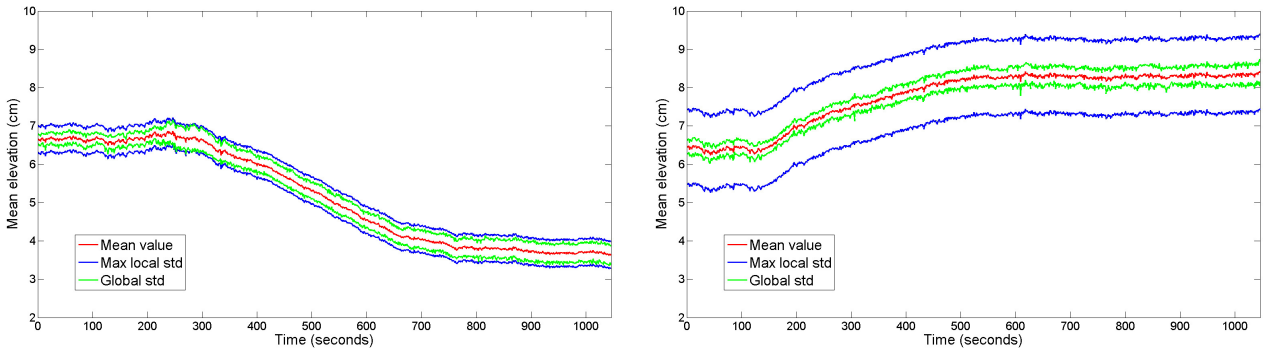

Fig. 7 Mean elevation of the detected bed lines over time with maximum local standard deviation and global standard deviation during the infiltration of fine beads of 0.7 mm (left) and 4 mm (right).

4.1 Channel slope evolution

One main purpose that motivated the development of the described image processing algorithm was to evaluate the influence of fine sediment size on the sediment mobility of the bed. Studying the channel slope over time is one way of doing that. The calculation of the channel slope was based on the bed line detection results. The line between the upper extremity of the outlet stopper and the mean bed height positioned in the middle of each image was considered. The slope of this straight line was defined as the channel slope. The slope was calculated on each image of all sequences in order to compare them. In Fig. 8, we can see the evolution of the channel slope for all of the sequences, each using a different size of fine particle. The channel slope with fine particles of size 0.7 mm, 0.9 mm, 1.5 mm and 2 mm decreased, indicating that the channel bed degraded. This degradation can be explained by the fine particles filling the interstices of the bed, enhancing the exposure of the coarse particles to the flow, therefore increasing their mobility. Conversely, when the fine component was formed of 4 mm beads, the channel aggraded (increasing the channel slope).

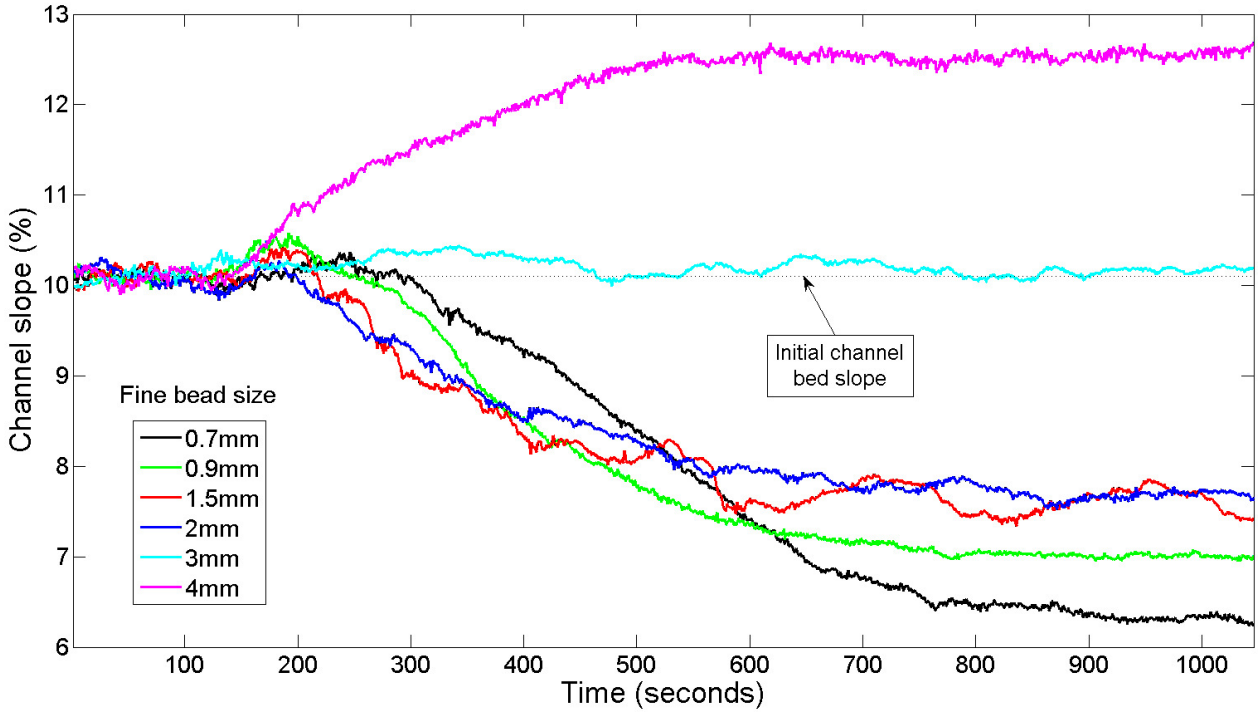

Fig. 8 Evolution of channel slope over time according to the size of fine sediment. The dotted line represents the initial channel bed slope at equilibrium, so at 10.1 %.

4.2 Water depth evolution

Another objective of this study was to examine the evolution of water depth during the fine sediment introduction period and see the influence of the fine sediment size. In Fig. 9, we can see the evolution of water depth over time for all sequences. It appears clearly that the smaller the fine beads, the higher the water depth. This can partly be explained by the reduction of slope when finer sediment is introduced. However, there may also be an opposite effect of fine sediment on the flow resistance.

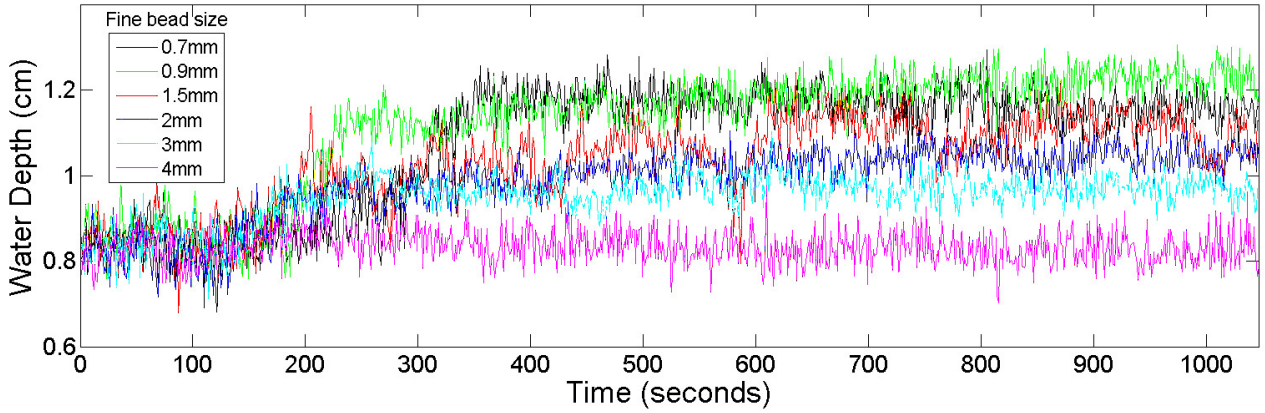

Fig. 9 Evolution of water depth over time according to fine sediment size.

5 Conclusion

In this paper, we have presented a novel approach for analysing bedload mobility in a laboratory experiment with image processing based algorithms. We used an inclined channel in which sediment and water supplies at the inlet were controlled accurately. A bimodal sediment mixture was obtained by feeding one-sized coarse beads of 5 mm and then one-sized fine beads of variable size across experiments (0.7 mm, 0.9 mm, 1.5 mm, 2 mm, 3 mm and 4 mm). Each experiment was filmed with a camera and gave a temporal sequence of images. Image processing was used as it enabled us to automatically detect features on images, and to deal with a large number of images. Our approach relies on the use of simple morphological operations such as closing, dilating, filtering and more advanced ones like gradient calculation and watershed transformation. Combining them, we were able to detect lines separating distinct regions on images: the base support, the mobile bed, the water flow and the air. These lines allow us to study the evolution of channel slope and water depth over time, and to conclude that grain size ratio has an important influence upon the bedload mobility.

As perspectives, the flow resistance could be studied by exploiting water depth evolution. Also, other experiments with different fine particle rates could be done to evaluate the influence of fine sediment feed concentration on both slope and water depth.

Acknowledgements. This research was supported by *Irstea* (formerly *Cemagref*), by the French *Institut National des Sciences de l'Univers* programme EC2CO-BIOHEFECT, by the *Natural Sciences and Engineering Research Council of Canada* (NSERC) and by the *Rhône-Alpes* region as part of its higher education, research and innovation regional strategy (*Environment Academic Research Community*).

References

[1] Frey, P., Church, M. (2011). Bedload: a granular phenomenon. *Earth Surface Processes and Landforms*, 36(1), pp 58-69. doi: 10.1002/esp.2103

[2] Parker, G., Klingeman, P. C. (1982). On why gravel bed streams are paved. *Water Resources Research*, 18(5), pp 1409-1423. doi: 10.1029/WR018i005p01409

[3] Thomas, N. (2000). Reverse and intermediate segregation of large beads in dry granular media. *Physical Review E*, 62(1), pp 961. doi: 10.1103/PhysRevE.62.961

[4] Hergault, V., Frey, P., Métivier, F., Barat, C., Ducottet, C., Böhm, T., Ancey, C. (2010). Image processing for the study of bedload transport of two-size spherical particles in a supercritical flow. *Experiments in fluids*, 49(5), pp 1095-1107. doi: 10.1007/s00348-010-0856-6

[5] Böhm, T., Frey, P., Ducottet, C., Ancey, C., Jodeau, M., Reboud, J. L. (2006). Two-dimensional motion of a set of particles in a free surface flow with image processing. *Experiments in fluids*, 41(1), pp 1-11. doi: 10.1007/s00348-006-0134-9

[6] Beucher, S., Lantuéjoul, C. (1979). Use of watersheds in contour detection. *In International Workshop on Image Processing, Real-Time Edge and Motion Detection*, Rennes, France, Sept.17-21

[7] Beucher, S., Meyer, F. (1992). The morphological approach to segmentation: the watershed transformation. *Optical Engineering-New York-Marcel Dekker Incorporated*, 34, pp 433-433

[8] Vincent, L., Soille, P. (1991). Watersheds in digital spaces: an efficient algorithm based on immersion simulations. *IEEE Transactions on Pattern Analysis and Machine Intelligence*, 13(6), pp 583-598. doi: 10.1109/34.87344

[9] Sobel, I., Feldman, G. (1968). A 3x3 isotropic gradient operator for image processing. *Presented a talk at the Stanford Artificial Intelligence Project*

[10] Beucher, S., Bilodeau, M. (1994). Road segmentation and obstacle detection by a fast watershed transformation. *In Intelligent Vehicles' 94 Symposium*, pp 296-301

[11] Patras, I., Hendriks, E. A., Lagendijk, R. L. (2001). Video segmentation by MAP labeling of watershed segments. *IEEE Transactions on Pattern Analysis and Machine Intelligence*, 23(3), pp 326-332. doi: 10.1109/34.910886

[12] Grau, V., Mewes, A. U. J., Alcaniz, M., Kikinis, R., Warfield, S. K. (2004). Improved watershed transform for medical image segmentation using prior information. *IEEE Transactions on Medical Imaging*, 23(4), pp 447-458. doi: 10.1109/TMI.2004.824224